Interpretable Force Perturbations Promote Gait Variability Without Affecting Perceived Exoskeleton Transparency

Alex van den Berg, Katherine L. Poggensee, *Member, IEEE*, David Abbink, *Senior Member, IEEE*, and Laura Marchal-Crespo, *Member, IEEE*

***Abstract*— Force perturbations during gait training can increase movement variability, which may support motor exploration and learning. However, when such perturbations are delivered through a robotic exoskeleton, they can also reduce perceived exoskeleton transparency, potentially hindering user acceptance. We tested whether visualizing continuous upper leg-level perturbations in immersive virtual reality (VR) could preserve their variability-enhancing effect while mitigating the cost to perceived transparency in a pelvis-centered walking task. Thirty healthy adults walked on a treadmill while wearing a robotic exoskeleton and performed a ball-in-cup task, requiring continuous mediolateral control of the pelvis. Participants trained under one of three conditions: Control (no perturbations), Perturbation (continuous noise-like multisine forces applied at the thighs), or Perturbation + Visual (same forces with a real-time, body-referenced force-beam visualization). Step-width variability was evaluated during Training. Task performance, intrinsic motivation, and perceived transparency were assessed across Baseline, Training, Retention, and a faster-speed Transfer test (120 % of preferred speed). Both perturbation conditions significantly increased step-width variability during Training relative to Control, with no detectable difference between Perturbation and Perturbation + Visual. Task performance improved from Baseline to Retention and Transfer across all conditions, with no significant differences across conditions. Motivation did not differ between conditions either. Critically, perceived transparency decreased only in the non-visualized Perturbation condition and remained stable in both Control and Perturbation + Visual. Our results show that continuous leg-level perturbations reliably enrich lateral gait variability and that simple visual force cues can prevent a perceived transparency cost without compromising the variability manipulation. Future work should test adaptive dosing, multisession training, and clinical cohorts with impaired lateral stability.**

***Index Terms*— Gait, perturbations, force visualization, step-width variability, virtual reality.**

I. Introduction

A HEALTHY gait enables us to move through diverse environments and situations seemingly effortlessly. A key mechanism supporting this capacity is the subtle step-to-step fluctuation in walking, known as gait variability [1]. Rather than being mere noise, evidence indicates that motor variability serves functional roles in exploration, adaptation, and robust control of movement [2], [3], [4]. Such variability enables adjustments to changing environmental and physiological conditions and can facilitate the learning of stable, efficient gait strategies [1], [5]. Therefore, instead of reducing variability through, e.g., robotic assistance [6], recent gait training and rehabilitation approaches suggest strategically increasing variability during gait training [2], [7].

One way to increase variability during gait training is to apply force perturbations. Gait perturbations can be delivered in various ways: treadmill belt accelerations [8], [9], visual-field shifts [10], [11], or forces applied by a wearable robot [12], [13], [14]. For instance, random pulse-like forces improved learning in a stepping-like task [13], and varied pelvis perturbations increased gait variability and enhanced functional outcomes in individuals with incomplete spinal cord injury [12]. However, improvements in learning are not always observed across force perturbation-based protocols. When such forces are delivered through an exoskeleton, perturbations can make it feel as if the user has to "fight" the robot, reducing *perceived transparency*, here defined as the user's subjective experience of how little the device resists or distorts self-generated movement [15]. Prior work has shown that force perturbations can diminish the sense of agency, i.e., the feeling of being in control of one's own movements [16], [17], or reduce motivation [18], which may ultimately hinder training engagement and motor learning [14], [19].

Received 9 January 2026; revised 7 April 2026; accepted 22 April 2026. Date of publication 27 April 2026; date of current version 10 June 2026. Associate Editor: Yanggang Feng. This work was supported by European Union's Horizon 2022 Marie Skłodowska-Curie Actions (MSCA) Postdoctoral Fellowship under Grant 101106071. *(Corresponding author: Alex van den Berg.)*

Alex van den Berg is with the Cognitive Robotics (CoR) Department, Delft University of Technology, 2628 CD Delft, The Netherlands (e-mail: alex_van_den_berg@hotmail.com).

Katherine L. Poggensee and Laura Marchal-Crespo are with the Cognitive Robotics (CoR) Department, Delft University of Technology, 2628 CD Delft, The Netherlands, and also with the Erasmus Medical Centre, 3015GD Rotterdam, The Netherlands.

David Abbink is with the Cognitive Robotics (CoR) Department and the Sustainable Design Engineering Department, Delft University of Technology, 2628 CD Delft, The Netherlands.

This article has supplementary downloadable material available at https://doi.org/10.1109/TNSRE.2026.3687639, provided by the authors.

Digital Object Identifier 10.1109/TNSRE.2026.3687639

One way to address this limitation is to add visual cues that provide information about the applied forces/torques, e.g., where they are applied on the body and their magnitude. The visualization of assisting forces has been shown to improve user acceptance and performance across different domains, likely by making them easier to understand [20], [21]. We theorize that visualizing force perturbations may mitigate the negative impact on user experience in perturbation-based training without compromising their augmenting effects on movement variability, thereby enhancing motor learning. In this work, we seek to achieve this by making upper-leg-applied-force perturbations legible but not predictable to the user by visualizing their current direction and magnitude in (immersive) Virtual Reality (VR).

To test this idea, we implemented the force visualization in an immersive VR motor-learning experiment using a novel gait task. Participants walked on a treadmill while balancing a virtual ball in a cup that moved laterally with their pelvis. The ball rolls without slipping, so keeping it in the cup requires participants to smoothly regulate their mediolateral pelvic motion while walking. The task draws on the everyday challenge of carrying an object that demands continuous lateral postural regulation, such as a cup of liquid [22], [23], with the key difference that in our task the cup motion is amplified and directly coupled to pelvis displacement, turning lateral pelvis regulation into an explicit, ongoing performance objective.

Mediolateral walking stability relies on the regulation of foot placement based on the state of the pelvis and center of mass [24], [25], [26], and step-width variability reflects the active control of this loop [27], [28]. Because variability along task-relevant dimensions is thought to be most beneficial for learning [29], [30], [31], and step-width variability is task-relevant for lateral stability [27], [32], enriching it during training may promote more adaptive balance control. The ball-in-cup task challenges this control dimension, providing a controlled testbed for studying whether continuous perturbations can improve its regulation. We implemented perturbations that continuously changed, noise-like forces applied to the upper legs using a customized treadmill-based robotic exoskeleton [33].

This approach differs from existing gait-perturbation programs that emphasize *reactive* responses to discrete events such as sudden belt accelerations (e.g., [8], [9]) or visual-field shifts (e.g., [10], [11]). Such training can improve reactive balance and reduce falls, yet its effects on steady-state gait quality are not consistently superior to conventional treadmill training [8], [34]. Our approach instead targets *proactive*, continuous regulation of lateral stability.

We run a parallel design experiment with thirty unimpaired participants, who trained the ball-in-a-cup task under either of three conditions: (i) without perturbation (Control), (ii) with force perturbations, and (iii) with force perturbations that were also visualized. We tested four hypotheses:

- H1: Force perturbations increase step-width variability during training compared with Control, while no differences are expected between the two perturbation conditions (i.e., with and without visualization);
- H2: Training with the perturbations improves retention and transfer of the pelvis-control task w.r.t. Control;
- H3: The visualization of the perturbation forces prevents the negative impact of perturbations on motivation and perceived transparency expected with non-visualized perturbations;
- H4: Since the disturbance visualization mitigates the motivation and perceived-transparency cost of perturbations without diminishing variability (H1–H3), this condition yields larger gains in task performance than training with non-visualized perturbations.

II. Methods

A. Participants

Thirty healthy participants (15 female, 15 male) took part in this study, with a mean age of 30.20 years ($SD = 6.80$), height of 1.80 m ($SD = 0.09$), and body mass of 83.27 kg ($SD = 14.91$). Most participants (27) had completed higher education, and 3 had completed secondary education. Prior VR experience varied: 6 had never used VR, 18 reported approximately 10 hours, 5 reported approximately 100 hours, and 1 reported more than 100 hours. Eight participants reported being prone to motion sickness. The mean preferred treadmill walking speed was 0.67 m/s ($SD = 0.10$). The study was approved by the Human Research Ethics Committee of Delft University of Technology (approval number: 5077) and conducted in compliance with the Declaration of Helsinki.

B. Experimental Setup

Participants walked on a treadmill while wearing a grounded exoskeleton, a modified version of the commercial Lokomat® (Hocoma AG, Switzerland), and an HTC Vive Pro Eye HMD (HTC Corporation, Taiwan). Limb motion was tracked with five Vive 3.0 trackers: one on the waist, two on the mid-feet, and two on the thigh straps near the knees (Fig. 1). Three additional trackers were mounted to the treadmill deck to define the world reference system. Three base stations covered the volume above the treadmill. The experiment was conducted on a Windows 10 (Microsoft, USA) machine with an NVIDIA GeForce RTX 3080 GPU, 32 GB of DIMM DDR4 memory, and an Intel Core i9-10850K CPU (Intel, USA).

1) Virtual Environment: The virtual environment was built in Unity 2022.3.23f1 and depicted a natural valley extending in the walking direction [35] (Fig. 1). We targeted a 90 Hz rendering rate to match the HMD's refresh rate. A translucent, treadmill-sized rectangle was rendered on the ground to help participants judge foot placement. Forward translation of the scene was synchronized to treadmill speed via User Datagram Protocol (UDP). In Fig. 1 bottom-right, we overlay the left-handed coordinate frame with x (mediolateral), y (vertical), and z (forward) axes, matching the coordinate frame in Unity. A semi-transparent heads-up display (HUD) was centered 3.5 m ahead and included a top-down view of the avatar's legs.

The lower-limb avatar (https://readyplayer.me/, 2023) was matched to each participant's size. In particular, the avatar height and leg length were adjusted using the HMD and waist

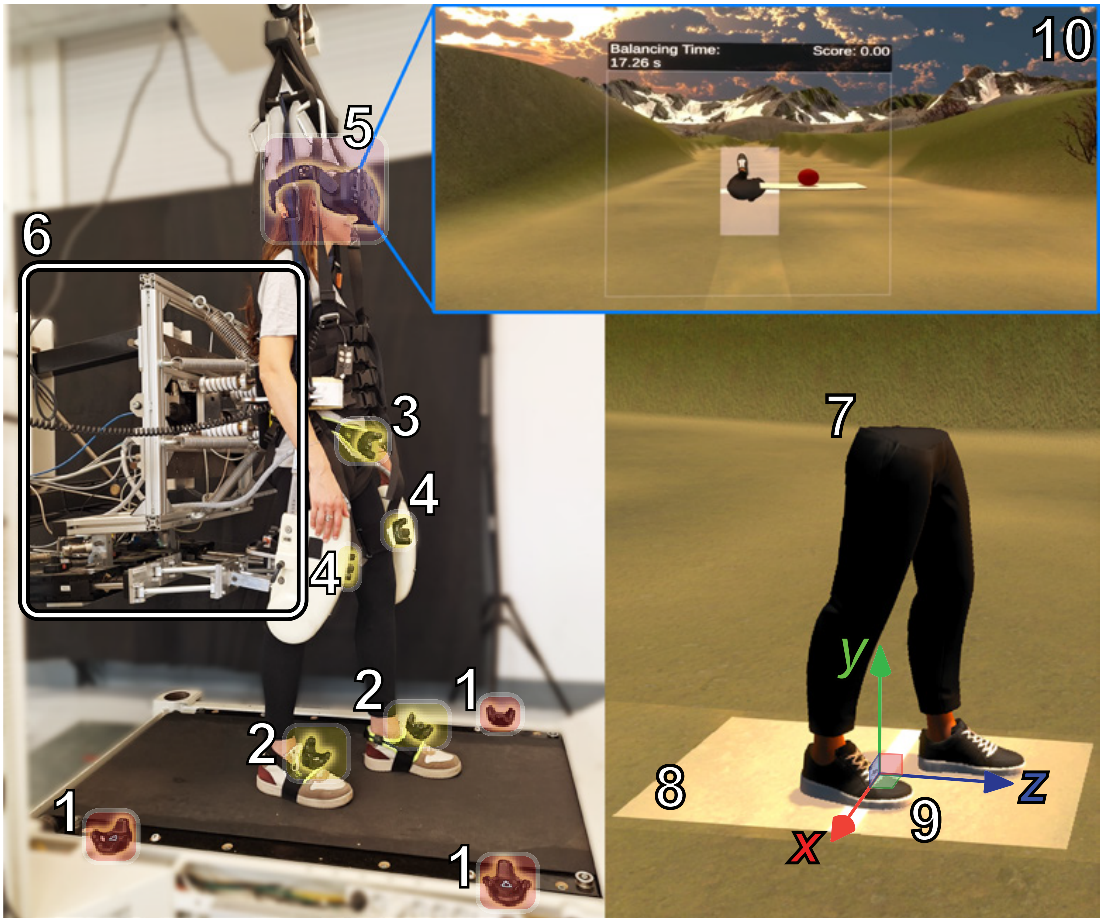

Fig. 1. **Experimental setup and virtual scene.** Left: participant instrumented for the experiment, showing (1) treadmill-mounted Vive trackers, (2) foot trackers, (3) waist/pelvis tracker, (4) exoskeleton thigh cuffs with co-located trackers, (5) head-mounted display, and (6) exoskeleton–MUCDA system. Right: virtual scene showing (7) avatar legs, (8) treadmill-aligned ground rectangle, (9) coordinate frame (x right, y up, z forward), and (10) first-person view with heads-up display.

tracker. Inverse kinematics (FinalIK v2.3, RootMotion) were used to animate the avatar's legs, based on the information from the waist, foot, and knee trackers.

2) Grounded Exoskeleton: The exoskeleton provides actuation for hip flexion/extension and abduction/adduction through two linear actuators per leg, arranged in a parallel, closed-chain mechanism. The system also includes a six-degree-of-freedom compliant pelvis module, with actuated lateral movement provided by a series elastic actuator (Fig. 1, left). The kinematics and actuator–joint mapping of the hip module are described in detail in [33]. Although the original device also supports knee actuation, the shank/knee assemblies were removed as delivering forces at the thighs was sufficient to increase mediolateral variability. Leaving the lower legs free simplified donning/doffing and reduced setup time.

The robot was operated in transparency mode, i.e., controlled to minimize resistance to self-generated movement [15]. Low-level control for the hip actuators was implemented in MATLAB/Simulink (R2013b) and compiled for the Simulink Real-Time (xPC) target, running at 1000 Hz. The linear actuators were commanded in force mode: the desired actuator force combined (i) a configuration-dependent gravity-compensation term, and (ii) a velocity-proportional friction-compensation term. The perturbation forces described in Subsection II-D were superimposed on top of these transparency-enhancing commands.

The MUltidimensional Compliant Decoupled Actuator (MUCDA) [36] was employed at the pelvis level. Lateral interaction force was estimated from the measured spring deflection, with stiffness k_s = 3379 N/m, along the mediolateral axis, as reported in [36]. The lateral actuator was commanded to cancel the estimated interaction force, whereas the remaining degrees of freedom remained passively compliant.

Virtual soft stops were implemented near the travel limits of both the hip and lateral pelvis actuators. The lateral pelvis actuator allowed a total motion of 0.20 m, with soft stops beginning at 0.08 m from the treadmill center. The soft-stop fields at the hip actuators engaged within 0.02 m from either end of the 0.40 m stroke. Within these boundary regions, any commanded transparency and perturbation forces that would drive the actuator further toward its limit were smoothly faded to zero.

The overhead body-weight support (BWS) harness was adjusted to support the exoskeleton's weight and provide fall protection. The BWS overhead carriage was coupled to the lateral motion of the pelvis module so that the harness attachment point followed the participant's mediolateral movement.

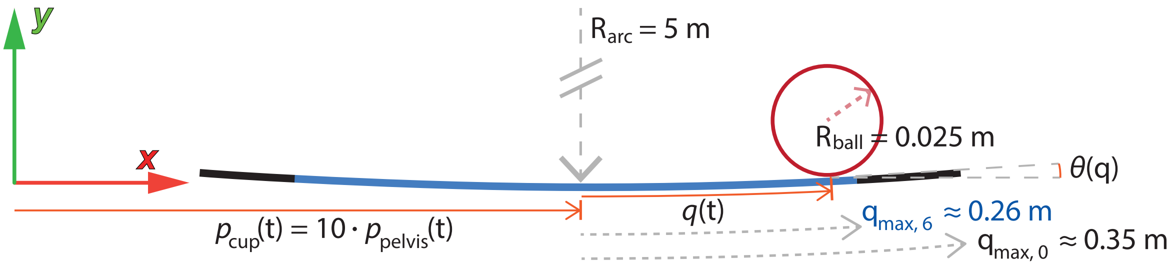

Fig. 2. **Schematic for the ball–cup system.** The cup is a circular arc (R_{arc} = 5 m) that translates laterally ($p_{cup}(t)$) with the pelvis ($p_{pelvis}(t)$). The ball moves along the arc with arc-length coordinate $q(t)$; $\theta(q)$ is the local tangent angle. The maximum arc-length to the edge depends on difficulty: at Level 0 (8°), $q_{max,0} \approx 0.35$ m; at Level 6 (6°), $q_{max,6} \approx 0.26$ m.

C. The Ball-in-Cup Task

Participants walked while balancing a virtual ball in a shallow cup that translated laterally with their pelvis (Fig.s 1 and 2). The (left-handed) world coordinate frame in Unity consists of x mediolateral, y vertical, and z forward directions. The cup was placed in front of the participant at (y, z) = (1.38 m, 2.0 m) so that both the task and the HUD were comfortably visible in the forward view while walking.

The cup was modeled as a circular arc of radius R_{arc} = 5 m, translating along the x-axis with the pelvis (Fig. 2). Mediolateral pelvis displacement relative to the center of the treadmill, $p_{pelvis}(t)$, was measured by the pelvis module and proportionally mapped to the cup center position:

$$p_{cup}(t) = k_{pc}\, p_{pelvis}(t), \qquad k_{pc} = 10. \tag{1}$$

The proportional gain was tuned so that typical pelvic excursions during walking produced clearly visible, but not excessive, cup motion, keeping the task centered in front of the participant and aligned with the HUD.

The ball was treated as a point mass constrained to move along the cup surface in the (x, y)-plane. Its position along the arc was parameterized by the arc-length coordinate $q(t)$ (in m), and the angle $\theta(q)$ between the tangent of the cup surface at the ball-cup contact point and the horizontal (in rad) (Fig. 2). Projecting forces onto the local tangent yielded:

$$\ddot{q} = -g\sin\theta(q) - \ddot{p}_{cup}\cos\theta(q) - \mu_d g\cos\theta(q)\mathrm{sgn}(\dot{q}) - d\dot{q}, \tag{2}$$

with gravity $g = 9.81$ m/s^2, Coulomb friction coefficient μ_d = 0.03, and viscous damping d = 0.8 /s. We approximated $\dot{p}_{cup}$ and $\ddot{p}_{cup}$ by finite differences. We then updated the ball states $(q, \dot{q})$ with an explicit Euler step at $\Delta t \approx 0.011$ s (matching the 90 Hz rendering rate).

R_{arc} was chosen so that the ball–cup natural frequency lay below typical stride frequencies (< 0.3 Hz). Then, μ_d and d were tuned so that the frequency response was relatively flat between 0.4 Hz to 3 Hz. This avoided resonances at walking-related frequencies while yielding dynamics that were challenging but achievable.

The ball was rendered with a radius (2.5 cm), and the visible edge of the cup was inset by the same amount so that a fall occurred when the ball appeared to pass over the edge. At the start of each trial, the ball spawned 1.0 m higher than the cup at $p_{cup} = 0$, hovered for 1.0 s, and then fell under gravity. If the ball missed the cup or later rolled over the edge, it continued to fall for 0.5 s and then reappeared at the starting location.

Task difficulty was controlled by the cup arc angle, expressed to participants as the task *Level*. During the Baseline, Retention, and Transfer phases, we used a fixed intermediate arc angle of 6° (Level 6). Throughout the Training phase, the angle varied between 8° (easier) and 5° (harder), as shown in Section II-F. Fig. 2 illustrates two example levels.

During the task, the HUD displayed a running *Balancing Time* and cumulative *Score*, with one point awarded for each second that the ball remained in the cup. The pelvis position was streamed from the exoskeleton controller to Unity over UDP at 90 Hz. Occasional packet loss was handled by linearly interpolating pelvis velocity and integrating Eq. 2 for each missing frame.

D. Perturbation Forces

When perturbations were active, the exoskeleton applied continuously varying forces to each leg through the thigh cuffs. We defined two perturbation *channels* per leg: a mediolateral (left–right) channel and an anteroposterior (front–back) channel. These channels were used to shape and visualize the perturbations in the virtual environment, aligned with the world x and z axes, respectively. However, we note that the applied forces were only approximately aligned with the fixed world-frame axes, due to the hardware configuration.

For each leg and channel, we generated a multisine signal:

$$s_{x,z}(t) = \sum_{i=1}^{150} A_i \sin\left(2\pi f_i t + \varphi_i\right), \tag{3}$$

with f_i uniformly spaced over [0.01, 0.5] Hz. Amplitudes $A_i \in [0.5, 1.0]$ and phases $\varphi_i \in [0, 2\pi)$ were drawn at random. For each participant, four independent realizations (two channels per leg) were generated using different random seeds. Each realization was normalized by its own nominal variance (Eq. 4) so that the resulting perturbation drive signals had matched power across all participants and conditions.

We then computed the nominal variance of each multisine:

$$\sigma^2 = \tfrac{1}{2}\sum_{i=1}^{150} A_i^2 \tag{4}$$

and used it to normalize and clamp the signals to [−1, 1]:

$$\hat{m}_{x,z}(t) = \max\left(-1,\ \min\left(1,\ \frac{s_{x,z}(t)}{2\sigma^2}\right)\right). \tag{5}$$

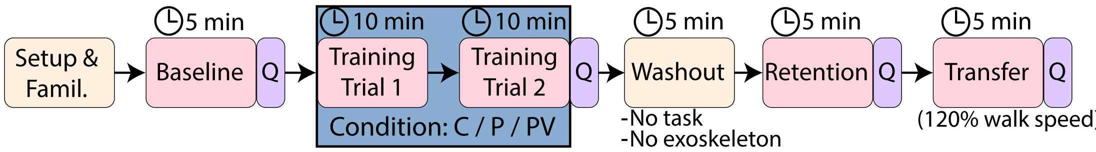

Fig. 3. **Experimental protocol.** After familiarization, participants completed Baseline (5 m), two 10 m Training blocks (under either Control, Perturbation, or Perturbation + Visual conditions), Washout (5 m), Retention (5 m), and Transfer (5 m at 120 % speed). Questionnaires (*Q*) were administered after each phase (see Section II-H).

These signals $\hat{m}_{x,z}(t)$ were then passed through a first-order low-pass filter with cutoff frequency $f_c = 0.525$ Hz to obtain smoothed perturbation drive signals $\tilde{m}_{x,z}(t)$.

We then defined the desired force perturbation components for each participant as:

$$F^{\text{req}}_{x,z}(t) \;=\; k_F\, M\, \tilde{m}_{x,z}(t), \qquad k_F = 0.015 \text{ N/kg}, \tag{6}$$

where M is the participant's body mass in kg.

The desired force components were then mapped to small target hip-angle increments:

$$\Delta\phi_{x,z}(t) \;=\; k_\phi\, F^{\text{req}}_{x,z}(t), \qquad k_\phi = 0.03 \text{ rad/N}, \tag{7}$$

interpreted as target increments in abduction/adduction (mediolateral channel) or flexion/extension (anteroposterior channel).

Let $\boldsymbol{\phi}$ denote the hip angles and $\boldsymbol{\phi}_{\text{cmd}}(t) = \boldsymbol{\phi}(t) + \Delta\boldsymbol{\phi}(t)$ the commanded angles after adding the perturbation increments from Eq. 7. Using the kinematic model of the exoskeleton [33], $\boldsymbol{\phi}_{\text{cmd}}(t)$ was mapped to desired actuator lengths $\boldsymbol{\ell}_{\text{cmd}}(t)$. The actuator commands were then generated as:

$$\boldsymbol{u}_{\text{pert}}(t) \;=\; k_P\big(\boldsymbol{\ell}_{\text{cmd}}(t) - \boldsymbol{\ell}_{\text{current}}(t)\big), k_P = 1500 \text{ N/m} \tag{8}$$

and superimposed on the transparency-mode commands (see Section II-B2). The gains k_F, k_ϕ, and k_P were tuned jointly during pilot testing to produce perturbations that reliably increased step-width variability across all participants, while remaining comfortable and preserving a sense of agency and safety during walking. To contextualize the calculated perturbation forces, for a 100 kg participant, the resulting actuator commands correspond to commanded peak perturbation forces on the order of 25 N per channel.

E. Perturbation Visualization

To visualize the perturbations in VR, we rendered an animated *force beam* anchored at the avatar's thigh trackers (Fig. 4). The beam extended toward a colored sphere, with direction and length determined from the smoothed normalized perturbation drives ($\tilde{m}_{x,z}(t)$). Beams were color-coded by leg (left: blue, right: orange) and particles flowed toward the sphere, indicating the direction in which the perturbation "pulled" the thigh.

The beam endpoint in the horizontal plane was calculated as:

$$\boldsymbol{d}_{\text{leg}}(t) \;=\; L_{\max}\, \tilde{\boldsymbol{m}}_{\text{leg}}(t), \qquad L_{\max} = 2.5 \text{ m}, \tag{9}$$

where $\tilde{\boldsymbol{m}}_{\text{leg}}(t) = \left[\tilde{m}_x(t), \tilde{m}_z(t)\right]^\top$, i.e., the filtered, normalized and clamped signal calculated in Eq. 5. The same beams were mirrored on the HUD (Fig. 1) so participants could perceive the perturbations from a frontal view without needing to look down at their legs.

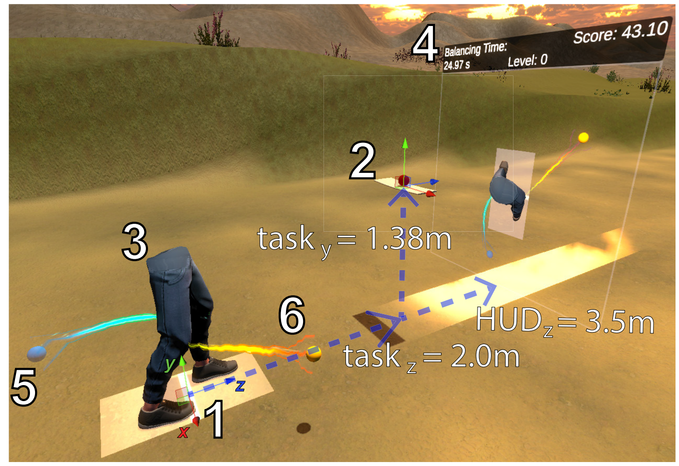

Fig. 4. **Perturbation visualization.** Labels: (1) scene origin; (2) pelvis-linked cup (at $p_{\text{cup}} = 0$); (3) avatar; (4) heads-up display; (5) left-leg force beam; (6) right-leg force beam. Beams were also mirrored on the HUD.

F. Experimental Protocol

After obtaining informed consent, we collected demographic information (see Section II-A). Body mass was measured using a standard scale and used to scale the perturbing forces (Eq. 6). Participants completed four main experimental phases in a single session, namely Baseline, Training, Retention, and Transfer, as illustrated in Fig. 3. They were pseudo-randomly assigned in equal numbers to one of three training conditions, with gender balanced across conditions:

1) **Control (C)**: no perturbation forces.
2) **Perturbation (P)**: perturbation forces applied during Training (see Subsection II-D).
3) **Perturbation + Visual (PV)**: Same as **P** with the addition of the force visualization (see Subsection II-E)

Before the main phases, participants completed **setup and familiarization**: we explained the experiment, fitted the trackers and harness, and calibrated the exoskeleton and avatar. Preferred treadmill speed was set during a 3 m walk with the HMD and exoskeleton. Participants then walked 5 m without the exoskeleton, 5 m with it, and practiced the ball-in-cup task for 3 m while standing. During standing practice, the experimenter explained the task goal (keep the ball on the platform by controlling pelvis motion). The task was active and visible on the screen, and participants were instructed to try it while the experimenter answered any questions. Exact instructions per phase can be found in the Supplementary Materials.

The **Baseline** started immediately after familiarization. Participants walked for 5 m at their preferred speed while performing the ball-in-cup task, providing baseline performance for all subsequent comparisons. Right after, participants received training condition-specific instructions and familiarization while standing for 2 m. Participants in the P and PV groups experienced the perturbing forces; those in PV also saw the visualization of the force beams (Subsection II-E).

The **Training** phase consisted of two 10 m walks, separated by a short break to mitigate fatigue. We chose 10 m blocks based on pilot testing, which indicated that this duration provided sufficient time to challenge participants and allow adaptation without excessive fatigue. During training, participants walked at their preferred speed while performing the ball-in-cup task under their assigned condition (C, P, PV).

Task difficulty was manipulated during training by changing the cup arc angle. Baseline, Retention, and Transfer used a fixed 6° setting. During training, the arc angle decreased from 8° to 5° over each 10 m block (ten discrete levels). This range was selected based on pilot participants: 6° caused the ball to leave the cup every few steps, and starting at 8° ensured most participants could initially keep the ball in the cup. We chose to vary the difficulty like this during training so that each participant spent time across a range of difficulties, increasing the chance that everyone experienced some practice time near their individual optimal challenge level, while keeping the protocol comparable across participants.

A 5 m **Washout** phase followed Training, during which participants walked without the exoskeleton or task to dissipate short-term after-effects. The **Retention** phase followed the same structure as Baseline. The **Transfer** test repeated the task at 120 % of preferred speed to evaluate performance transfer at a faster, albeit typical, treadmill speed, in line with prior gait studies [37], [38].

Between phases, participants stepped out of the exoskeleton and removed the HMD, which provided a brief seated rest to reduce fatigue. After each experimental phase (Baseline, the two Training blocks, Retention, and Transfer), they completed the Intrinsic Motivation Inventory [39] and the perceived-transparency questionnaire (Subsection II-H) on a monitor. The total session, including setup, familiarization, walking phases, and questionnaires, lasted approximately 120 m.

G. Data Processing

All time-stamped tracker and HMD poses, as well as system and task states (see Section II-C) were logged in Unity at 90 Hz using the Unity Experimental Framework [40]. Questionnaires were administered outside of VR on a monitor using the VR Questionnaire Toolkit [41].

We detected steps using a coordinate-based algorithm validated for treadmill walking [42]. We determined each foot's position relative to the hip tracker along the z-axis, filtered it (zero-phase fourth-order Butterworth, 5 Hz cutoff), and identified local maxima corresponding to heel strikes. Timestamps were refined by identifying when foot velocity fell below 0.1 m/s.

Occasional tracking noise led to erroneous detection of heel strikes, i.e., the time and position of the heel strike instances could not be accurately detected due to tracker inaccuracies. Using a custom interface (detailed in the Supplementary Materials), we manually identified and removed 1417 such erroneously detected steps in total (mean 5.95 per walk, $SD = 3.69$), leaving an average of 394.67 steps ($SD = 33.45$) per 5 m walk.

H. Outcome Metrics

Task performance. To evaluate how well participants performed the ball-in-cup task, we employed the *mean normalized margin (distance) to the cup edge* as a performance metric. Let $q(t)$ be the ball's arc-length coordinate along the cup surface and let $q_{\max}$ be the arc-length from the center to the cup edge (as defined in Subsection II-C and Fig. 2). The instantaneous normalized edge margin is then defined as:

$$e(t) = 1 - \frac{|q(t)|}{q_{\max}}. \tag{10}$$

Note that $e(t) \in [0, 1]$ while the ball is in the cup, with $e = 1$ at the center and $e = 0$ at the edge. For each phase/training block, we computed the average $\bar{e}$ over all samples when the ball was in the cup.

A caveat is that this metric only partially relates to the instruction to keep the ball in the cup. However, the number of ball drops showed pronounced ceiling effects after the training, limiting sensitivity to between-condition differences. Complete results for the number of ball drops are reported in the Supplementary Materials.

Gait variability. We evaluated step-width variability as our gait-variability outcome due to its role in regulating pelvis control in the mediolateral direction [24], [26]. Step width was defined as the absolute mediolateral (along the x axis) distance between consecutive heel strikes. For each phase or training block and leg, we computed the standard deviation of the step width over all valid steps (after filtering) and averaged the two legs to obtain a single measure of step-width variability. Left and right legs were calculated separately and then averaged to avoid inflating variability due to potential asymmetry.

Motivation. We assessed participants' intrinsic motivation after the Baseline, Training, Retention, and Transfer phases using a selected group of items from the Intrinsic Motivation Inventory (IMI) [39]. Four questions from three IMI subscales were selected for their relevance to this study, namely interest/enjoyment, perceived competence, and effort. Each item was rated on a 7-point Likert scale. Scores were averaged across items (after reverse-coding if applicable).

Perceived transparency. We assessed participants' perceived transparency of the exoskeleton interaction after Baseline, Training, Retention, and Transfer using a short questionnaire adapted from previous exoskeleton–transparency work [43]. The six items were:

- How much resistance was the exoskeleton giving to your movements? (from [44])
- How comfortable were the movements while walking in the exoskeleton? (from [45])

- It seemed like I was in control of the exoskeleton. (from [46])
- It seemed like I was causing the movements of the exoskeleton. (from [46])
- How natural could you walk with the exoskeleton?
- It seemed as if the exoskeleton was controlling me. (from [46])

Responses were on a 7-point Likert scale. The first and last items were reverse-coded so that higher values indicated better perceived transparency. We report the mean of all six items as a composite score for perceived transparency.

I. Statistical Analysis

All outcome metrics were analyzed with linear mixed models (LMMs) in R (v4.4.0) using `lme4`, `lmerTest` (Kenward–Roger degrees of freedom), `emmeans`, and `ggplot2`. Fixed effects included the training *Condition* (Control, Perturbation, Perturbation + Visual) and the within-subject *Phase*, plus their interaction. Subject-specific (*ID*) random effects accounted for repeated measurements. The employed model had the form:

$$Out \sim \text{Condition} \times \text{Phase} + (1 + \text{taskCount} \mid \text{ID}), \quad (11)$$

where *taskCount* indexes how many times the ball-in-cup task had been performed up to that point (Baseline = 1; Training 1 = 2; Training 2 = 3; Retention = 4; Transfer = 5).

For the analysis of the step-width variability (H1), we focused on how Training changed gait variability relative to Baseline. The model, therefore, included Baseline and both 10 m Training blocks (Phase = Baseline, Training), with the two Training blocks entered as separate observations under the same Phase label. For three participants, one Training block showed substantial drift in the foot-tracking data and was excluded from this analysis (P: Training 1 and Training 2; PV: Training 1). To evaluate changes in task performance (normalized edge margin, $\bar{e}$) after training (H2 & H4), we included Baseline, Retention, and Transfer in *Phase*. Further, to address the hypothesis related to motivation and perceived transparency (H3), we modeled participants' subjective ratings using Baseline and Training *Phase* only.

The model took the Control condition and Baseline phase as reference levels. Two-sided tests used $\alpha = 0.05$, and Kenward–Roger degrees of freedom were reported for fixed effects. Holm correction was applied to all p-values within each analysis. When the Condition×Phase interaction was significant, or to answer specific hypotheses, i.e., H4, we used `emmeans` to compute the planned within-condition contrasts. Model diagnostics included residual Q–Q and residual-versus-fitted plots, convergence checks, and screening for singular or boundary random-effects fits. Further, to support interpretation of non-significant between-condition contrasts, we performed post-hoc sensitivity and Bayesian follow-up analyses.

III. Results

A. Effect of Perturbations on Step-Width Variability (H1)

We found that continuous leg-level perturbations significantly increased lateral gait variability during training (Fig. 5).

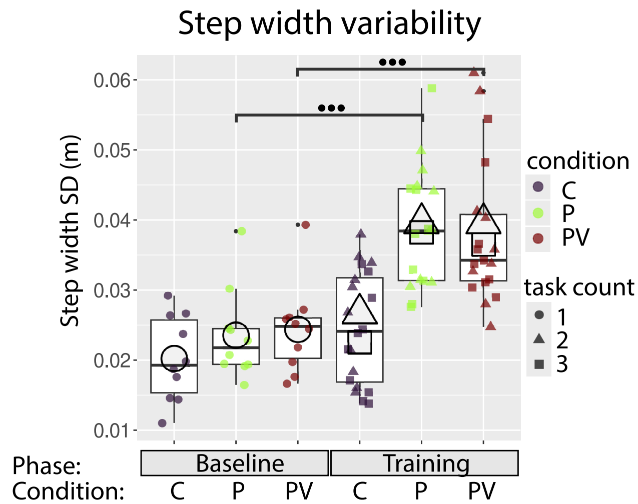

Fig. 5. **Step-width variability at Baseline and Training.** Standard deviation of step width for Control (C), Perturbation (P), and Perturbation + Visual (PV) for Baseline and Training phases. Small points represent individual participants; different colors indicate the condition, and different shapes indicate the task count: Baseline, Training 1, and Training 2. Large symbols show the mean for each task count group for that condition and phase. Boxplots indicate median and IQR (whiskers = 1.5 IQR). Horizontal bars mark significant contrasts (••• $p_{\text{Holm}} < 0.001$).

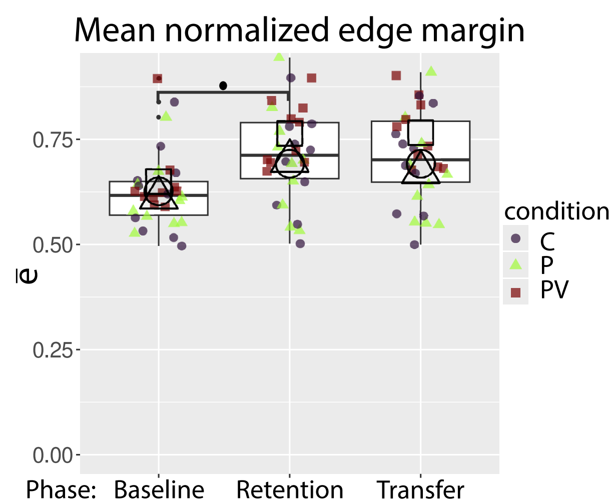

Fig. 6. **Task performance across phases.** Mean normalized edge margin $\bar{e}$ (0 at edge, 1 at center) for Control (C), Perturbation (P), and Perturbation + Visual (PV) for Baseline, Retention, and Transfer phases. Small points represent individual participants; different shapes and colors indicate the condition. Large symbols show the mean for each condition for that phase. Boxplots indicate median and IQR (whiskers = 1.5 IQR). Horizontal bar marks significant contrast (• $p_{\text{Holm}} < 0.05$).

In the mixed model, Training-related changes depended on Condition: the Condition×Training interaction terms were significant for both Perturbation (estimate $\beta = 0.0116$ m, $t(52.27) = 4.06$, $p_{\text{Holm}} = 0.001$, $d = 2.47$) and Perturbation + Visual ($\beta = 0.0104$ m, $t(51.54) = 3.66$, $p_{\text{Holm}} = 0.002$, $d = 2.22$), whereas the main effect of Training alone was small and nonsignificant ($p_{\text{Holm}} = 1.0000$). Post hoc analysis revealed no significant difference between the two perturbation groups ($p_{\text{Holm}} = 0.694$).

TABLE I

LINEAR MIXED MODEL RESULTS FOR TASK PERFORMANCE. THE OUTCOME IS THE NORMALIZED EDGE MARGIN $\bar{e}$. P = PERTURBATION; PV = PERTURBATION + VISUAL; *SE* = STANDARD ERROR; DF = KENWARD–ROGER DEGREES OF FREEDOM; d = EFFECT SIZE (COHEN'S d-TYPE). WE REPORT UNCORRECTED AND HOLM-CORRECTED p-VALUES; ITALICS INDICATE $0.05 < p_{\text{HOLM}} \leq 0.10$, BOLD INDICATES $p_{\text{HOLM}} < .05$

Effect	Estimate	SE	df	t	p	p_{Holm}	d
(Intercept)	0.1639	0.0073	30.23	22.48	<0.001	<0.001	22.32
Condition: P	−0.0039	0.0103	30.23	−0.38	0.705	1.000	−0.54
Condition: PV	0.0061	0.0103	30.23	0.60	0.555	1.000	0.84
Phase: Retention	0.0172	0.0050	44.83	3.45	0.001	**0.010**	2.34
Phase: Transfer	0.0171	0.0060	31.43	2.87	0.007	*0.051*	2.33
P × Retention	0.0057	0.0070	44.83	0.81	0.421	1.000	0.78
PV × Retention	0.0128	0.0070	44.83	1.82	0.075	0.452	1.75
P × Transfer	−0.0013	0.0084	31.43	−0.15	0.879	1.000	−0.18
PV × Transfer	0.0133	0.0084	31.43	1.58	0.125	0.626	1.81

B. Effect of Conditions on Task Performance (H2 & H4)

We found a general significant improvement in task performance after training (Table. I, Fig. 6). In particular, the normalized edge margin significantly increased from Baseline to Retention ($p_{\text{Holm}} = 0.010$) and showed a smaller, near-significant increase from Baseline to Transfer ($p_{\text{Holm}} = 0.051$).

We did not find significant effects of the *Condition* and the *Condition*×*Phase* interaction. The post-hoc analysis to answer H4 did not result in significant differences between the Perturbation and Perturbation + Visual conditions (Retention: $p_{\text{Holm}} = 1.000$; Transfer: $p_{\text{Holm}} = 0.549$). A sensitivity analysis indicated that, with the present sample and variance structure, the study had 80% power to detect standardized between-condition effects of approximately $d = 0.40$ at Retention and $d = 0.48$ at Transfer. Observed effect sizes were substantially smaller ($d = 0.02$–0.27), suggesting limited power to reliably detect small effects. Bayesian follow-up analyses provided moderate evidence in favor of the null for Perturbation versus Control at Retention ($BF_{01} = 4.95$), Perturbation versus Control at Transfer ($BF_{01} = 5.53$), and Perturbation + Visual versus Perturbation at Retention ($BF_{01} = 4.26$). For the remaining contrasts, evidence was anecdotal ($BF_{01} = 1.65$–2.02), so small condition differences cannot be ruled out.

C. Effect of Visualization on Motivation and Perceived Transparency (H3)

For the experimental conditions studied, motivation scores were not impacted by the condition, phase, or their interaction; post-hoc comparisons between perturbation conditions did not yield significant differences ($p_{\text{Holm}} = 0.504$). Perturbation versus Control and Perturbation + Visual versus Control gave moderate BF_{01} support for the null, whereas Perturbation + Visual versus Perturbation was inconclusive.

Perceived transparency showed a different pattern (Fig. 7). Here, the Condition×Training interaction reached significance for the Perturbation group ($\beta = -1.02$, $t(30) = -3.05$, $p_{\text{Holm}} = 0.024$, $d = -1.93$), but not for PV ($p_{\text{Holm}} = 0.933$). Post-hoc analysis indicates that perceived transparency did not significantly change in the Control ($p_{\text{Holm}} = 0.446$) and PV groups ($p_{\text{Holm}} = 0.803$) between Baseline and Training, but significantly decreased in the Perturbation group ($\Delta = -0.71$, $t(33.33) = -2.85$, $p_{\text{Holm}} = 0.022$). For the non-significant between-condition contrasts, PV versus Control showed moderate BF_{01} support for the null, whereas PV versus Perturbation was inconclusive.

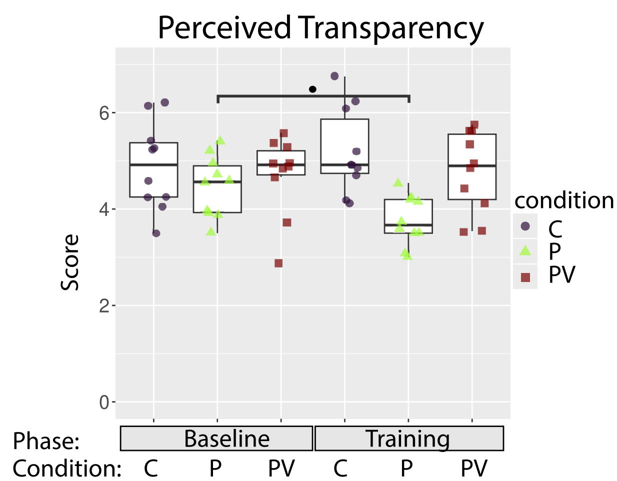

Fig. 7. **Perceived transparency results.** Composite scores for Control (C), Perturbation (P), and Perturbation + Visual (PV) for Baseline and Training phases. Points represent individual participants; different shapes and colors indicate the condition. Boxplots indicate median and IQR (whiskers = 1.5 IQR). Horizontal bar marks significant contrast (• $p_{\text{Holm}} < 0.05$).

IV. DISCUSSION

We tested whether continuous leg-level perturbations, and visualizing them in VR, could increase lateral gait variability during Training (H1), translating into better retention and transfer of a pelvis-control task (H2), without hampering motivation or perceived transparency compared with non-visualized perturbations (H3). We further hypothesized that visualizing perturbations would yield greater performance benefits than perturbations without visualization (H4).

A. Perturbations Increased Gait Variability (H1)

As hypothesized, both perturbation conditions significantly increased step-width variability during training compared to Baseline, whereas Control did not. These results confirm that the noise-like thigh-level perturbations successfully increased variability along this task-relevant dimension (Section II-C).

Importantly, adding the force visualization did not reduce the perturbation-induced increase in step-width variability.

Baseline step-width variability was approximately 26 mm (SD of step width), consistent with a previous treadmill-VR study from our group [35]. The perturbations increased step-width variability by roughly 40–45% relative to Baseline, a substantially larger effect than the $\approx$ 15% increase from subtle avatar-foot disturbances in our previous study [35], though more comparable to the increases reported for larger visual-field perturbations [11]. A pre-task familiarization walk without the exoskeleton or task produced similar step-width variability (see Supplementary Materials), suggesting that neither altered baseline lateral gait variability. Whether this magnitude of variability enrichment falls within a productive range to enhance learning is discussed in next section (Section IV-B).

B. Task Performance Improved After Training, Regardless of the Training Condition (H2 & H4)

In general, all participants improved their performance on the pelvis-control task from Baseline to Retention and Transfer. Bayesian follow-up analyses provided moderate null support for several between-condition contrasts, while others remained inconclusive (see Section III). Thus, we did not find robust evidence that force perturbations benefited task performance compared to the Control group, even though these conditions *did* enhance gait variability (see H1). Several factors may explain why the variability enrichment confirmed in H1 did not translate into task-performance advantages. First, more variability does not necessarily mean better learning. In a redundant bimanual task, moderate variability increases ($\approx$ 40%) left learning intact, whereas doubling variability impaired retention [47]. Our 40–45% increase falls near the upper end of this tolerable range [2], [47]. At such levels, the motor system may struggle to consolidate what it has practiced [31]. Second, perturbation parameters were fixed across participants and throughout the session, despite large individual differences in baseline performance, meaning some participants were likely under-challenged and others over-challenged. Third, exploration is most valuable early in learning and should taper as a solution is found [4], [30], whereas our fixed dose did not allow this.

Beyond the variability–learning relationship, measurement, and design factors may have further limited our ability to detect condition-specific advantages. All participants were trained for a relatively long time, possibly achieving their maximum attainable skill level (ceiling effect) and thereby overshadowing any potential benefits of variability-enriched practice. Additionally, although our primary metric $\bar{e}$ was chosen to avoid the clear ceiling effects observed in drop-based measures (see Supplementary Materials), it does not directly quantify failures. Participants may have prioritized avoiding drops and, once that goal was met, tolerated the ball drifting closer to the edge to make walking more comfortable. This mismatch likely reduced our ability to detect condition-specific advantages. Finally, we observed large variability in skill level among participants, which inflates between-participant variability and reduces sensitivity to between-condition differences in performance changes.

We also did not observe condition-specific advantages in the Transfer test at 120 % of preferred speed, despite walking faster generally altering stability margins [38], [48], [49]. Beyond the measurement-related limitations noted above, the Transfer task may have remained too similar to the training situation. Transfer tasks that more strongly alter the walking context, such as overground walking [8], [12], [34], or that involve obstacle-negotiation scenarios (e.g., navigating a crowd [50]), may be better suited to reveal any added value of variability-enriched training.

C. The Visualization of the Forces Mitigated the Negative Effects of the Perturbations on Perceived Transparency (H3)

We did not observe a significant decrease in motivation when perturbations were added during Training, even without visualization, which contradicts prior literature [18], [19]. This may reflect the engaging, game-like nature of the ball-in-cup task and immersive VR setting. Individual differences in preference for challenge could moderate how perturbations affect motivation and should be examined in future adaptive-difficulty schemes.

Perceived transparency showed a clearer pattern. Participants in the non-visualized Perturbation condition (P) reported a reduction in perceived transparency from Baseline to Training, whereas perceived transparency did not change significantly in either the Control or PV groups, despite the latter group experiencing similar perturbation forces. A possible interpretation, in line with prior work showing that unexplained or poorly understood forces can degrade trust and user acceptance [51], [52], [53], is that perturbations accompanied by interpretable, body-referenced visual information are easier to understand and accept. This is supported by findings that visualizing interaction forces can improve user acceptance [20], [21]. It is plausible that the force beams helped participants contextualize that their legs were being perturbed, even though the perturbations remained unpredictable.

From a motor learning perspective, our results are promising: variability-enriching perturbations need not come at the cost of reduced perceived transparency when accompanied by interpretable feedback. This may be particularly relevant for multisession interventions or for clinical populations, where maintaining transparency and motivation is important for training adherence, and where discomfort may further constrain what perturbation doses are acceptable [15], [54], [55].

D. Limitations

Several limitations should be considered when interpreting these findings. First, all assessments were performed in a single session on the same day with healthy, young adults walking on a treadmill in VR. The study therefore cannot speak to long-term learning or consolidation effects, and it remains unknown whether the observed effects would extend over multisession training with longer-term retention tests. Moreover, the ecological validity of the ball-in-cup task as a proxy for real-world gait stability has not been established. We did not assess transfer to overground walking or functional measures (e.g., fall risk, walking endurance), so whether the results would generalize beyond the treadmill-VR setting or translate to populations with impaired lateral stability remains an open question.

Second, perceived transparency was assessed only with self-report questionnaires, which limits the interpretation of our results. Future work should combine self-reports with objective measures—e.g., interaction forces, surface Electromyography (sEMG)—to help explain the mechanism behind the observed differences in perception, e.g., if the reduction of perceived transparency was accompanied by an increase of muscle co-contraction measured through sEMG, known to regulate movement variability [56].

Third, task difficulty and perturbation strength were held constant across participants, despite substantial variability in baseline performance. This likely meant that some participants were under-challenged and others over-challenged, which can diminish the differences in learning conditions. Additionally, our primary performance metric captured the mean distance from the cup edge while the ball was in the cup. Although this choice avoided the strong ceiling effects in drop-based measures, it only partially matched the verbal instruction and may not fully reflect skill improvements.

Fourth, the perturbations were generated and commanded in actuator space and then interpreted as mediolateral and antero-posterior components aligned with the virtual world frame. Because the linear actuators pivot with the leg, the actual forces at the thigh cuffs were always applied along the actuator axes. Additionally, since we did not perform a cuff-level force calibration, the reported force magnitudes are model-based estimates. Finally, the modest sample size (30 participants across three conditions) and substantial baseline variability likely reduced sensitivity to subtle between-condition differences, consistent with the inconclusive Bayesian follow-up results for some contrasts. Smaller or participant-specific effects may become clearer with larger samples and individualized dosing.

E. Implications and Future Work

First, continuously varying leg-level perturbations provide a reliable means to increase lateral gait variability during treadmill walking, while participants can still improve a pelvis-centered control task over practice. The combination of a pelvis-linked task and noise-like leg perturbations provides a controlled testbed for studying proactive, continuous regulation of mediolateral stability, complementing traditional paradigms that primarily train reactive responses [8], [34]. The task also enforces external attention, which can enhance motor learning [57], [58]. Under the present single-session protocol, however, this approach has not yet translated into clear task-performance advantages over Control.

Second, visualizing the perturbations in an interpretable, body-referenced manner prevented the reduction in perceived transparency seen with non-visualized perturbations, while preserving the increase in step-width variability. When designing variability-enriching perturbations for training or rehabilitation, adding an interpretable visualization may help maintain comfort and perceived agency without needing to weaken the perturbations themselves [40], [59], [60].

To support reproducibility and future extensions, we provide the complete experimental dataset, all analysis code, and the Unity assets (ball-in-cup task, perturbation visualization, signal generation) as open resources (see Section V).

Future work should build on these points in several directions. Methodologically, adaptive difficulty and perturbation dosing could be implemented to keep the task appropriately challenging for each participant, for example, by adjusting cup arc angle, damping, and pelvis-to-cup gain (Eq. 1) based on ongoing performance and, potentially, individual characteristics such as preference for challenge [61]. Such schemes would not only target an individually optimal challenge level but also enable outcome metrics, such as the highest level of difficulty maintained without drops, that may be less prone to ceiling effects than fixed-level performance measures. Experimentally, extending the protocol to multiple training sessions, adding longer-term retention tests, incorporating more challenging transfer tasks (e.g., overground walking, narrow-base walking, or obstacle negotiation), and analyzing more detailed dynamic stability metrics and step-to-step structure will help clarify whether variability-enriched, pelvis-centered training can yield durable gains in gait adaptability and deepen our understanding of how these perturbations affect gait control. Clinically, testing this approach in populations with impaired lateral stability (e.g., older adults at risk of falls or individuals after stroke) will be an important next step. The ball-in-cup task may itself have value as a training tool: it provides continuous feedback on pelvis regulation, is intuitive, and its difficulty can be adjusted parametrically. Combined with the perturbation and visualization components, it could serve as a platform for pelvis-centered gait training in which difficulty, variability enrichment, and feedback are each tailored to the individual. Whether this can meaningfully improve functional walking outcomes remains to be tested.

F. Conclusion

This study set out to examine whether continuously varying leg-level force perturbations can be used to strategically enrich gait variability during a pelvis-centered VR walking task, and whether visualizing those perturbations can preserve user experience while maintaining the effectiveness of the variability manipulation. We found that the perturbations reliably increased step-width variability during training, and adding visualization did not diminish this effect. The perturbation visualization prevented the reduction in perceived transparency that occurred when perturbations were applied without visual feedback, supporting the idea that making externally applied forces more interpretable can mitigate user-experience costs. For several key contrasts, Bayesian analysis provided moderate evidence against differential learning effects between conditions; for others, the evidence was inconclusive, and small effects cannot be excluded. We did not observe clear perturbation-related advantages in improving the pelvis-centered VR walking task after training within this single-session protocol.

Together, a pelvis-linked control task, noise-like leg perturbations, and interpretable force visualization provide a foundation for variability-based gait training that preserves perceived transparency. Although variability enrichment alone was not sufficient here to yield superior task learning, future work with adaptive dosing, multisession training, and more challenging transfer tasks may clarify when and how this approach translates into more robust, generalizable gait control.

V. Data Availability

The complete experimental dataset, all analysis code, a demonstration video, and instructions for reproducing their analyses are publicly available on Zenodo (https://doi.org/10.5281/zenodo.17414637). In addition, this article has supplementary downloadable material available at https://doi.org/10.1109/TNSRE.2026.3687639, comprising a detailed pdf document with additional methodological details, Simulink models, Unity and signal-generation assets, questionnaire item lists, and extended statistical results to support deeper insight, reproducibility, and future extensions of this work.

Acknowledgment

The authors sincerely thank Hocoma AG for their invaluable assistance and for providing access to the Lokomat® treadmill and safety harness system used in this study and Alberto Garzás Villar for his assistance with the statistical analyses.

References

[1] J. T. Cavanaugh and N. Stergiou, "Gait variability: A theoretical framework for gait analysis and biomechanics," in *Biomechanics and Gait Analysis*. Amsterdam, The Netherlands: Elsevier, 2020, pp. 251–286.

[2] N. Stergiou, R. T. Harbourne, and J. T. Cavanaugh, "Optimal movement variability: A new theoretical perspective for neurologic physical therapy," *J. Neurologic Phys. Therapy*, vol. 30, no. 3, pp. 120–129, 2006. [Online]. Available: https://journals.lww.com/jnpt/fulltext/2006/09000/optimal_movement_variability__a_new_theoretical.6.aspx

[3] S. J. Harrison and N. Stergiou, "Complex adaptive behavior and dexterous action," *Nonlinear Dyn.*, vol. 19, no. 4, pp. 345–94, 2015. [Online]. Available: https://www.ncbi.nlm.nih.gov/pmc/articles/PMC4755319/

[4] D. Sternad, "It's not (only) the mean that matters: Variability, noise and exploration in skill learning," *Current Opinion Behav. Sci.*, vol. 20, pp. 183–195, Apr. 2018.

[5] S. W. Ducharme and R. E. A. van Emmerik, "Fractal dynamics, variability, and coordination in human locomotion," *Kinesiol. Rev.*, vol. 7, no. 1, pp. 26–35, Feb. 2018. [Online]. Available: https://journals.humankinetics.com/view/journals/krj/7/1/article-p26.xml

[6] J. De Miguel-Fernández, J. Lobo-Prat, E. Prinsen, J. M. Font-Llagunes, and L. Marchal-Crespo, "Control strategies used in lower limb exoskeletons for gait rehabilitation after brain injury: A systematic review and analysis of clinical effectiveness," *J. NeuroEngineering Rehabil.*, vol. 20, no. 1, p. 23, Feb. 2023. [Online]. Available: https://link.springer.com/article/10.1186/s12984-023-01144-5

[7] T. G. Hornby, J. Moore, C. L. Holleran, and C. E. Henderson, "Taking the next step in neurologic rehabilitation: Contributions of intensity and variability of stepping tasks during locomotor training," *Phys. Therapy*, vol. 105, no. 3, pp. 49–100, Mar. 2025, doi: 10.1093/ptj/pzaf005.

[8] M. M. Rieger, S. Papegaaij, F. Steenbrink, J. H. van Dieën, and M. Pijnappels, "Effects of perturbation-based treadmill training on balance performance, daily life gait, and falls in older adults: REACT randomized controlled trial," *Phys. Therapy*, vol. 104, no. 1, pp. 1–10, Jan. 2024, doi: 10.1093/ptj/pzad136.

[9] J. Li and H. J. Huang, "Small directional treadmill perturbations induce differential gait stability adaptation," *J. Neurophysiology*, vol. 127, no. 1, pp. 38–55, Jan. 2022. [Online]. Available: https://journals.physiology.org/doi/10.1152/jn.00091.2021

[10] E. B. Wilson, J. S. Bergquist, W. G. Wright, and D. A. Jacobs, "Gait stability in virtual reality: Effects of VR display modality in the presence of visual perturbations," *J. NeuroEngineering Rehabil.*, vol. 22, no. 1, pp. 1–15, Feb. 2025. [Online]. Available: https://jneuroengrehab.biomedcentral.com/articles/10.1186/s12984-025-01558-3

[11] P. M. McAndrew, J. M. Wilken, and J. B. Dingwell, "Dynamic stability of human walking in visually and mechanically destabilizing environments," *J. Biomechanics*, vol. 44, no. 4, pp. 644–649, Feb. 2011.

[12] J.-T. Lin, C.-J. Hsu, W. Dee, D. Chen, W. Z. Rymer, and M. Wu, "Varied movement errors drive learning of dynamic balance control during walking in people with incomplete spinal cord injury: A pilot study," *Exp. Brain Res.*, vol. 238, no. 4, pp. 981–993, Apr. 2020. [Online]. Available: https://link-springer-com.tudelft.idm.oclc.org/article/10.1007/s00221-020-05776-0

[13] L. Marchal–Crespo, J. Schneider, L. Jaeger, and R. Riener, "Learning a locomotor task: With or without errors?," *J. NeuroEngineering Rehabil.*, vol. 11, no. 1, pp. 1–10, Dec. 2014. [Online]. Available: https://link.springer.com/article/10.1186/1743-0003-11-25

[14] L. Marchal-Crespo, L. Michels, L. Jaeger, J. López-Olóriz, and R. Riener, "Effect of error augmentation on brain activation and motor learning of a complex locomotor task," *Frontiers Neurosci.*, vol. 11, p. 526, Sep. 2017. [Online]. Available: https://www.frontiersin.org/articles/10.3389/fnins.2017.00526/full

[15] N. Jarrasse and G. Morel, "Connecting a human limb to an exoskeleton," *IEEE Trans. Robot.*, vol. 28, no. 3, pp. 697–709, Jun. 2012. [Online]. Available: https://ieeexplore.ieee.org/abstract/document/6112804

[16] Ö. Özen, K. A. Buetler, and L. Marchal–Crespo, "Promoting motor variability during robotic assistance enhances motor learning of dynamic tasks," *Frontiers Neurosci.*, vol. 14, Feb. 2021, Art. no. 600059.

[17] W. Arink, K. L. Poggensee, N. Beckers, D. A. Abbink, and L. Marchal-Crespo, "Indirect haptic disturbances enhance motor variability, with divergent effects on skill transfer," in *Proc. 10th IEEE RAS/EMBS Int. Conf. Biomed. Robot. Biomechatronics (BioRob)*, Sep. 2024, pp. 1269–1274.

[18] L. Marchal–Crespo, P. Tsangaridis, D. Obwegeser, S. Maggioni, and R. Riener, "Haptic error modulation outperforms visual error amplification when learning a modified gait pattern," *Frontiers Neurosci.*, vol. 13, p. 61, Feb. 2019, doi: 10.3389/fnins.2019.00061.

[19] J. E. Duarte and D. J. Reinkensmeyer, "Effects of robotically modulating kinematic variability on motor skill learning and motivation," *J. Neurophysiology*, vol. 113, no. 7, pp. 2682–2691, Apr. 2015.

[20] A. van den Berg, J. Hofland, C. J. M. Heemskerk, D. A. Abbink, and L. Peternel, "Augmenting visual feedback with visualized interaction forces in haptic-assisted virtual-reality teleoperation," *Frontiers Robot. AI*, vol. 11, Dec. 2024, Art. no. 1427095.

[21] V. Ho, C. Borst, M. M. van Paassen, and M. Mulder, "Increasing acceptance of haptic feedback in UAV teleoperation by visualizing force fields," in *Proc. IEEE Int. Conf. Syst., Man, Cybern. (SMC)*, Oct. 2018, pp. 3027–3032.

[22] J. M. Bond and M. Morris, "Goal-directed secondary motor tasks: Their effects on gait in subjects with Parkinson disease," *Arch. Phys. Med. Rehabil.*, vol. 81, no. 1, pp. 110–116, Jan. 2000. [Online]. Available: https://www.sciencedirect.com/science/article/abs/pii/S0003999300902302

[23] M. Oh-Park, R. Holtzer, J. Mahoney, C. Wang, P. Raghavan, and J. Verghese, "Motor dual-task effect on gait and task of upper limbs in older adults under specific task prioritization: Pilot study," *Aging Clin. Experim. Res.*, vol. 25, no. 1, pp. 99–106, Apr. 2013. [Online]. Available: https://link.springer.com/article/10.1007/s40520-013-0014-0

[24] J. M. Donelan, D. W. Shipman, R. Kram, and A. D. Kuo, "Mechanical and metabolic requirements for active lateral stabilization in human walking," *J. Biomechanics*, vol. 37, no. 6, pp. 827–835, Jun. 2004. [Online]. Available: https://www-sciencedirect-com.tudelft.idm.oclc.org/science/article/pii/S0021929003003968

[25] A. L. Hof, M. G. J. Gazendam, and W. E. Sinke, "The condition for dynamic stability," *J. Biomechanics*, vol. 38, no. 1, pp. 1–8, Jan. 2005. [Online]. Available: https://www.sciencedirect.com/science/article/abs/pii/S0021929004001642

[26] M. Vlutters, E. H. F. Van Asseldonk, and H. Van der Kooij, "Center of mass velocity based predictions in balance recovery following pelvis perturbations during human walking," *J. Experim. Biol.*, vol. 219, no. 10, pp. 1514–1523, Jan. 2016, doi: 10.1242/jeb.129338.

[27] C. E. Bauby and A. D. Kuo, "Active control of lateral balance in human walking," *J. Biomechanics*, vol. 33, no. 11, pp. 1433–1440, Nov. 2000.

[28] A. D. Kuo and J. M. Donelan, "Dynamic principles of gait and their clinical implications," *Phys. Therapy*, vol. 90, no. 2, pp. 157–174, Feb. 2010, doi: 10.2522/ptj.20090125.

[29] H. G. Wu, Y. R. Miyamoto, L. N. G. Castro, B. P. Ölveczky, and M. A. Smith, "Temporal structure of motor variability is dynamically regulated and predicts motor learning ability," *Nature Neurosci.*, vol. 17, no. 2, pp. 312–321, 2014. [Online]. Available: https://www.nature.com/articles/nn.3616

[30] A. K. Dhawale, M. A. Smith, and B. P. Ölveczky, "The role of variability in motor learning," *Annu. Rev. Neurosci.*, vol. 40, no. 1, pp. 479–498, Jul. 2017. [Online]. Available: https://www.annualreviews.org/content/journals/10.1146/annurev-neuro-072116-031548

[31] R. Ranganathan and K. M. Newell, "Changing up the routine: Intervention-induced variability in motor learning," *Exercise Sport Sci. Rev.*, vol. 41, no. 1, pp. 64–70, 2013. [Online]. Available: https://journals.lww.com/acsm-essr/fulltext/2013/01000/changing_up_the_routine__intervention_induced.10.aspx

[32] J. S. Brach, J. E. Berlin, J. M. VanSwearingen, A. B. Newman, and S. A. Studenski, "Too much or too little step width variability is associated with a fall history in older persons who walk at or near normal gait speed," *J. NeuroEngineering Rehabil.*, vol. 2, no. 1, pp. 1–8, Dec. 2005. [Online]. Available: https://link.springer.com/articles/10.1186/1743-0003-2-21

[33] B. Luciani et al., "Personalized gait patterns during exoskeleton-aided training may have minimal effect on user experience. Insights from a pilot study," *IEEE Trans. Neural Syst. Rehabil. Eng.*, 2025. [Online]. Available: https://arxiv.org/html/2512.17425v1

[34] F. Hulzinga et al., "Repeated gait perturbation training in Parkinson's disease and healthy older adults: A systematic review and meta-analysis," *Frontiers Human Neurosci.*, vol. 17, Jun. 2023, Art. no. 732648.

[35] A. van den Berg, K. L. Poggensee, D. Abbink, and L. Marchal-Crespo, "Visual disturbances to avatar foot position increase step-width variability in immersive VR treadmill walking," *IEEE Trans. Neural Syst. Rehabil. Eng.*, vol. 33, pp. 2123–2134, 2025. [Online]. Available: https://ieeexplore-ieee-org.tudelft.idm.oclc.org/abstract/document/11004065

[36] D. Wyss, A. Pennycott, V. Bartenbach, R. Riener, and H. Vallery, "A MUltidimensional compliant decoupled actuator (MUCDA) for pelvic support during gait," *IEEE/ASME Trans. Mechatronics*, vol. 24, no. 1, pp. 164–174, Feb. 2019.

[37] S. Kim, M. Son, S. Shin, T. Kim, and S.-J. Choi, "Analysis of gait characteristics to evaluate injury risk after high-intensity exercise, focusing on canoe athletes: A preliminary study," *Frontiers Sports Act. Living*, vol. 7, Oct. 2025, Art. no. 1652610.

[38] J. Padulo, S. Rampichini, M. Borrelli, D. M. Buono, C. Doria, and F. Esposito, "Gait variability at different walking speeds," *J. Funct. Morphology Kinesiol.*, vol. 8, no. 4, p. 158, Nov. 2023. [Online]. Available: https://www.mdpi.com/2411-5142/8/4/158/htm

[39] R. M. Ryan, "Control and information in the intrapersonal sphere: An extension of cognitive evaluation theory," *J. Personality Social Psychol.*, vol. 43, no. 3, pp. 450–461, Sep. 1982.

[40] J. Brookes, M. Warburton, M. Alghadier, M. Mon-Williams, and F. Mushtaq, "Studying human behavior with virtual reality: The unity experiment framework," *Behav. Res. Methods*, vol. 52, no. 2, pp. 455–463, Apr. 2020. [Online]. Available: https://link.springer.com/article/10.3758/s13428-019-01242-0

[41] M. Feick, N. Kleer, A. Tang, and A. Krüger, "The virtual reality questionnaire toolkit," in *Proc. 33rd Annu. ACM Symp. User Interface Softw. Technol.*, Oct. 2020, pp. 68–69, doi: 10.1145/3379350.3416188.

[42] J. Zeni, J. G. Richards, and J. S. Higginson, "Two simple methods for determining gait events during treadmill and overground walking using kinematic data," *Gait Posture*, vol. 27, no. 4, pp. 710–714, 2007.

[43] S. D. Gasperina, A. L. Ratschat, and L. Marchal-Crespo, "Quantitative and qualitative evaluation of exoskeleton transparency controllers for upper-limb neurorehabilitation," in *Proc. Int. Conf. Rehabil. Robot. (ICORR)*, Sep. 2023, pp. 1–6.

[44] F. Just et al., "Exoskeleton transparency: Feed-forward compensation vs. disturbance observer," *Automatisierungstechnik*, vol. 66, no. 12, pp. 1014–1026, Dec. 2018. [Online]. Available: https://www.degruyterbrill.com/document/doi/10.1515/auto-2018-0069/html

[45] D. Verdel, G. Sahm, S. Bastide, O. Bruneau, B. Berret, and N. Vignais, "Influence of the physical interface on the quality of human-exoskeleton interaction," *IEEE Trans. Hum.-Mach. Syst.*, vol. 53, no. 1, pp. 44–53, Jan. 2023. [Online]. Available: https://ieeexplore.ieee.org/abstract/document/9786716

[46] I. V. Piryankova et al., "Owning an overweight or underweight body: Distinguishing the physical, experienced and virtual body," *PLoS ONE*, vol. 9, no. 8, Aug. 2014, Art. no. e103428. [Online]. Available: https://journals.plos.org/plosone/article?id=10.1371/journal.pone.0103428

[47] M. Cardis, M. Casadio, and R. Ranganathan, "High variability impairs motor learning regardless of whether it affects task performance," *J. Neurophysiology*, vol. 119, no. 1, pp. 39–48, 2017. [Online]. Available: https://journals.physiology.org/doi/10.1152/jn.00158.2017

[48] J. B. Dingwell and L. C. Marin, "Kinematic variability and local dynamic stability of upper body motions when walking at different speeds," *J. Biomechanics*, vol. 39, no. 3, pp. 444–452, Jan. 2006. [Online]. Available: https://www.sciencedirect.com/science/article/abs/pii/S0021929005000102?via%3Dihub

[49] D. D. Espy, F. Yang, T. Bhatt, and Y.-C. Pai, "Independent influence of gait speed and step length on stability and fall risk," *Gait Posture*, vol. 32, no. 3, pp. 378–382, Jul. 2010.

[50] P. Antonellis et al., "Gait during community ambulation and laboratory-based walking in people with mild traumatic brain injury," *Gait Posture*, vol. 117, pp. 254–260, Mar. 2025. [Online]. Available: https://www-sciencedirect-com.tudelft.idm.oclc.org/science/article/pii/S0966636225000025

[51] D. A. Abbink, M. Mulder, and E. R. Boer, "Haptic shared control: Smoothly shifting control authority?," *Cognition, Technol. Work*, vol. 14, no. 1, pp. 19–28, Mar. 2012.

[52] M. Itoh, F. Flemisch, and D. Abbink, "A hierarchical framework to analyze shared control conflicts between human and machine," *IFAC-PapersOnLine*, vol. 49, no. 19, pp. 96–101, 2016, doi: 10.1016/j.ifacol.2016.10.468.

[53] F. Flemisch, J. Kelsch, C. Löper, A. Schieben, and J. Schindler, "Automation spectrum, inner/outer compatibility and other potentially useful human factors concepts for assistance and automation," *Human Factors Assistance Autom.*, vol. 11, no. 2, pp. 45–67, May 2021.

[54] K. Oyake, K. Sue, M. Sumiya, and S. Tanaka, "Physical therapists use different motivational strategies for stroke rehabilitation tailored to an individual's condition: A qualitative study," *Phys. Therapy*, vol. 103, no. 6, pp. 1–10, Jun. 2023, doi: 10.1093/ptj/pzad034.

[55] C. McCrum et al., "Perturbation-based balance training: Principles, mechanisms and implementation in clinical practice," *Frontiers Sports Act. Living*, vol. 4, Oct. 2022, Art. no. 1015394. [Online]. Available: https://pmc.ncbi.nlm.nih.gov/articles/PMC9583884/

[56] J. A. Calalo et al., "The sensorimotor system modulates muscular co-contraction relative to visuomotor feedback responses to regulate movement variability," *J. Neurophysiology*, vol. 129, no. 4, pp. 751–766, Apr. 2023, doi: 10.1152/jn.00472.2022.

[57] L.-K. Chua, J. J. Díaz, R. Lewthwaite, T. Kim, and G. Wulf, "Superiority of external attentional focus for motor performance and learning: Systematic reviews and meta-analyses," *Psychol. Bull.*, vol. 147, no. 6, pp. 618–645, 2021.

[58] R. Lewthwaite and G. Wulf, "Optimizing motivation and attention for motor performance and learning," *Current Opinion Psychol.*, vol. 16, pp. 38–42, Aug. 2017. [Online]. Available: https://www-sciencedirect-com.tudelft.idm.oclc.org/science/article/pii/S2352250X1630152X

[59] P. S. Takazono, C. R. de Souza, J. Á. de Oliveira, D. B. Coelho, and L. A. Teixeira, "High contextual interference in perturbation-based balance training leads to persistent and generalizable stability gains of compensatory limb movements," *Exp. Brain Res.*, vol. 238, no. 5, pp. 1249–1263, May 2020. [Online]. Available: https://link.springer.com/article/10.1007/s00221-020-05806-x

[60] J. Lee and S. Choi, "Effects of haptic guidance and disturbance on motor learning: Potential advantage of haptic disturbance," in *Proc. IEEE Haptics Symp.*, Mar. 2010, pp. 335–342.

[61] A. Garzás-Villar et al., "The interplay between haptic guidance and personality traits in robotic-assisted motor learning," *J. NeuroEngineering Rehabil.*, vol. 22, no. 1, p. 238, Nov. 2025. [Online]. Available: https://link.springer.com/article/10.1186/s12984-025-01709-6